Spin Polarized Atomic Structure Calculations for 3d-Transition Atoms

Akira NARITA and Hideo KOBAYASHI*

(Received November 30, 1995)

The spin polarized atomic structure calculations are numerically performed for 3d-transition atoms with the configuration consistent with the experiments by uses of the exchange potentials due to Slater and Kohn-Sham and the exchange-correlation ones due to Barth-Hedin and Gunnarsson-Lundqvist. In these calculations, the energy levels, the potentials and the surface charge densities are computed in the self-consistent way, and compared for the various type exchange potentials. The followings are found. 1) The energy levels are very sensitive to the potentials and also the effects of exchange-correlation energies are large. 2) The spin polarization makes the total energy lower, and therefore this supports the strong magnetism due to the crystallization of the atom. 3) The frozen core approximation may be good for the 1s to 3p electrons when these atoms make the solids, but the spin polarized 3d to 4s electrons extend and will become to band electrons.

1. Introduction

It is very useful to grasp the electronic energy band structures for understanding the physical properties of the solids. We are interested in calculating the band structures. Although there are some calculating methods for them, we adopt the APW method since it gives the better agreement with the experiments [1, 2]. It is very convenient to know the physical properties of atoms constituting the solid, before we proceed to the band structure calculations. By knowing the properties such as the energy levels and the wave functions, we shall have a helpful direction for understanding the properties of the solids and for calculating their band structures.

For this reason, we here concentrate on the atomic structure calculations [4, 5, 13]. The results will be used for the band structure calculations, which will be carried out in another papers. The 3d-transition atoms from Sc to Cu are chosen for the purpose because they show strong magnetic properties. Accordingly, a purpose of this paper is to do the self-consistent atomic structure calculations for the 3d-transition atoms. In the calculations, the spin polarizations are taken into account and the effects of the various type exchange and exchange-correlation potentials due to Slater, Kohn-Sham, Barth-Hedin and Gunnarsson-Lundqvist on the energy levels and the wave functions are investigated and compared [4-6, 9, 10].

2. Theory

2.1 Local density approximation

We here first describe the total energy. The total energy of the electron system in an atom is given by [8]

$$E_{total} = \int d\boldsymbol{r} \sum_i \sum_\sigma \Psi^*_{i\sigma}(\boldsymbol{r}) \hat{f} \Psi_{i\sigma}(\boldsymbol{r}) + \frac{1}{2}\int d\boldsymbol{r}\rho(\boldsymbol{r}) V_c(\boldsymbol{r}) + \int d\boldsymbol{r}\rho(\boldsymbol{r}) \varepsilon_{xc}(\rho_\uparrow(\boldsymbol{r}), \rho_\downarrow(\boldsymbol{r})), \tag{1}$$

where

$$\hat{f} = -\nabla^2 - \frac{2Z}{r}, \tag{2}$$

$$V_c(\boldsymbol{r}) = \int \frac{\rho(\boldsymbol{r}')}{|\boldsymbol{r}-\boldsymbol{r}'|} d\boldsymbol{r}', \tag{3}$$

---

* Student of Akita National College of Technology

$$\rho_\sigma(\boldsymbol{r}) = \sum_i |\Psi_{i\sigma}(\boldsymbol{r})|^2, \tag{4}$$

$$\rho(\boldsymbol{r}) = \rho_\uparrow(\boldsymbol{r}) + \rho_\downarrow(\boldsymbol{r}), \tag{5}$$

Z is the atomic number, $V_c(\boldsymbol{r})$ is the Coulomb energy, $\rho_\sigma(\boldsymbol{r})$ is the charge density with spin σ, and $\varepsilon_{xc}(\rho_\uparrow(\boldsymbol{r}), \rho_\downarrow(\boldsymbol{r}))$ is the spin polarized exchange-correlation energy per one electron and its form will be given later. Below, we use the abbreviated notations ρ and ρ_σ ($\sigma = \uparrow, \downarrow$) instead of $\rho(\boldsymbol{r})$ and $\rho_\sigma(\boldsymbol{r})$. Here we use the approximation that the charge density ρ_σ is only a function of r and does not depend on the angular coordinates. Then, $V_c(r)$ becomes to the function of only r. The one-electron Schrödinger equation is given by

$$(-\nabla^2 + V_\sigma(r))\Psi_{i\sigma}(r) = E_{i\sigma}\Psi_{i\sigma}(r), \tag{6}$$

where

$$V_\sigma(r) = -\frac{2Z}{r} + V_c(r) + V_{xc}^{(\sigma)}(r). \tag{7}$$

Equation (6) is derived from the variation of $E_{total} - E_{i\sigma}N$ with respect to $\Psi_{i\sigma}^*(\boldsymbol{r})$, in which N is the total number of electrons given by integrating ρ and $E_{i\sigma}$ is the Lagrange multiplier [5] and the meaning is an energy eigenvalue. The exchange-correlation potential is given by

$$V_{xc}^{(\sigma)}(\boldsymbol{r}) = \frac{\partial}{\partial\rho_\sigma}[\rho\varepsilon_{xc}(\rho_\uparrow, \rho_\downarrow)]. \tag{8}$$

Thus, we regard the Coulomb and the exchange-correlation energies as the functionals of ρ_σ, and the Schrödinger equation is derived from variation occurred through the virtual small change of wave function. In the numerical calculations, we solve the equation. There, we use the locally varying charge density. This method is known as the local density approximation [7, 14]. Of course, we use this approximation in this paper. Using (1), (6) and (7) we get the total energy as follows [5]

$$\begin{aligned} E_{total} = {} & \sum_i \sum_\sigma n_{i\sigma}E_{i\sigma} - \frac{1}{2}\int d\boldsymbol{r}\rho(\boldsymbol{r})\, V_c(\boldsymbol{r}) \\ & - \int d\boldsymbol{r} \sum_\sigma \rho_\sigma(\boldsymbol{r})\, V_{xc}^{(\sigma)}(\boldsymbol{r}) \\ & + \int d\boldsymbol{r}\rho(\boldsymbol{r})\,\varepsilon_{xc}(\rho_\uparrow, \rho_\downarrow). \end{aligned} \tag{9}$$

The wave function $\Psi_{i\sigma}(\boldsymbol{r})$ can be written in the form $\Psi_{i\sigma}(\boldsymbol{r}) = R_{l\sigma}(r)\, Y_{lm}(\theta, \phi)$, in which $R_{l\sigma}(r)$ is the radial part and the principal quantum number is omitted, and $Y_{lm}(\theta, \phi)$ is the spherical harmonics. The Schrödinger equation for $R_{l\sigma}(r)$ is given by

$$-\frac{1}{r^2}\frac{d}{dr}\left(r^2\frac{dR_{l\sigma}}{dr}\right) + \left(V_\sigma(r) + \frac{l(l+1)}{r^2}\right)R_{l\sigma} = ER_{l\sigma}. \tag{10}$$

2.2 *Exchange-correlation energy*

We adopt four kinds of exchange and exchange-correlation potentials for $\varepsilon_{xc}(\rho_\uparrow, \rho_\downarrow)$, that is, Slater and Kohn-Sham exchange potentials, and Barth-Hedin and Gunnarsson-Lundqvist exchange-correlation potentials [5, 6, 9, 10]. Below, we use the abbreviated notations S and K-S instead of Slater and Kohn-Sham, and similarly use B-H and G-L instead of Barth-Hedin and Gunnarsson-Lundqvist.

First, we should refer to S and K-S exchange potentials since they have the similar form. S and K-S exchange potentials are well-known and given by

$$V_{xc}^{(\sigma)}(r) = V_x^{(\sigma)}(r) = -6\alpha\left(\frac{3}{4\pi}\rho_\sigma(r)\right)^{1/3}, \tag{11}$$

where $\alpha = 1$ for S and $\alpha = 2/3$ for K-S. From eqs. (8) and (11), $\varepsilon_x(\rho_\uparrow, \rho_\downarrow)$ can be written as follows

$$\varepsilon_x(\rho_\uparrow, \rho_\downarrow) = -\frac{9\alpha}{8\pi g r_s}[(1+\varsigma)^{4/3} + (1-\varsigma)^{4/3}], \tag{12}$$

where $g = (4/9\pi)^{1/3} = 0.52106176$, r_s is defined by $4\pi r_s^3/3 = 1/\rho$, and $\zeta = (\rho_\uparrow - \rho_\downarrow)/\rho$. For $\zeta = 0$, the paramagnetic state is realized and $\varepsilon_x = \varepsilon_x^{(p)} = -9\alpha/(4\pi g r_s)$. For $\zeta = 1$, the ferromagnetic state is realized and then $\varepsilon_x = \varepsilon_x^{(f)} = -9\alpha\cdot 2^{4/3}/(8\pi g r_s) = 2^{1/3}\varepsilon_x^{(p)}$. Using $\varepsilon_x^{(p)}$ and $\varepsilon_x^{(f)}$, $\varepsilon_x(\rho_\uparrow, \rho_\downarrow)$ becomes to

$$\varepsilon_x(\rho_\uparrow, \rho_\downarrow) = \varepsilon_x^{(p)} + (\varepsilon_x^{(f)} - \varepsilon_x^{(p)})f(\varsigma), \tag{13}$$

with

$$f(\varsigma) = \frac{1}{2(a-1)}[(1+\varsigma)^{4/3} + (1-\varsigma)^{4/3} - 2], \tag{14}$$

where $a = 2^{1/3}$, and $\varepsilon_x^{(p)} = (\varepsilon_x^{(f)} - \varepsilon_x^{(p)})/(a-1)$ is used.

Next we consider B-H exchange-correlation energy. It is given by

$$\varepsilon_{xc}(\rho_\uparrow, \rho_\downarrow) = \varepsilon_{xc}^{(p)}(r_s) + \eta(r_s)f(\varsigma), \tag{15}$$

$$\eta(r_s) = \varepsilon_{xc}^{(f)}(r_s) - \varepsilon_{xc}^{(p)}(r_s), \tag{16}$$

$$\varepsilon_{xc}^{(i)} = \varepsilon_x^{(i)} + \varepsilon_c^{(i)} \quad (i = p,f), \tag{17}$$

where $\varepsilon_x^{(i)}(r_s)$ is the K-S exchange energy and the value of α is 2/3, and $i = p$ and $i = f$ mean the paramagnetic and the ferromagnetic states, respectively. Here, $\varepsilon_c^{(i)}(r_s)$ is the correlation energy among many electrons, and can be written as

$$\varepsilon_c^{(i)}(r_s) = -c_i G(x_i), \tag{18}$$

where $x_i = r_s/r_i$, $c_p = 0.045$, $r_p = 21$ and $c_f = c_p/2 = 0.0225$, $r_f = 2^{4/3} r_p = 2\alpha r_p$ are chosen, and $G(x)$ is

$$G(x) = (1+x^3) \ln \left(1+\frac{1}{x}\right) - x^2 + \frac{x}{2} - \frac{1}{3}. \tag{19}$$

Note that the correlation energy $\varepsilon_c(\rho_\uparrow, \rho_\downarrow)$ is also given by the same form as $\varepsilon_x(\rho_\uparrow, \rho_\downarrow)$ denoted by eq. (13). For the paramagnetic state, this reduces to Hedin-Lundqvist exchange-correlation energy [11]. After a long calculation, we get the following B-H exchange potential

$$V_{xc}^{(\sigma)}(r_s) = V_0(r_s) + V_1(r_s)\left[(1+\sigma\varsigma)^{1/3} - 1\right] + V_2(r_s) f(\varsigma), \tag{20}$$

$$V_0(r_s) = -\frac{2}{\pi g r_s} - c_p \ln \left(1+\frac{1}{x_p}\right), \tag{21}$$

$$V_1(r_s) = -\frac{2}{\pi g r_s} + \frac{4}{3(a-1)}\left[c_p G(x_p) - c_f G(x_f)\right], \tag{22}$$

$$V_2(r_s) = c_p \ln \left(1+\frac{1}{x_p}\right) - c_f \ln \left(1+\frac{1}{x_f}\right) - \frac{4}{3}\left[c_p G(x_p) - c_f G(x_f)\right], \tag{23}$$

where $\sigma = 1$ for up spin and $\sigma = -1$ for down spin [10].

The G-L exchange-correlation potential is the same form as the B-H exchange-correlation potential only with the different constants given by $c_p = 0.0666$, $r_p = 11.4$ and $c_f = 0.0406$, and $r_f = 15.9$ [9].

3. Calculation method

The Schrödinger equation given by (10) must be solved numerically. For the numerical calculations, the well-known Numerov method is used. It is convenient to introduce the logarithmic variable given by $x = \ln r$ in the real calculations because the equation must be solved with high precision for very small r in order to guarantee sufficient accuracy for the whole r of the numerical solutions [5]. Putting $Y(x) = r^{1/2} R(r)$, we get the next equation instead of (10) [15]

$$Y''(x) = \gamma(x) Y(x), \tag{24}$$

$$\gamma(x) = e^{2x}\left[V(r) - E\right] + \left(l + \frac{1}{2}\right)^2. \tag{25}$$

The asymptotic behaviors of the solution are $Y(x) \propto e^{(l+1/2)x}$ for small x and $Y(x) \propto \exp(x/2 - \sqrt{-E}e^x)$ for large x. The equation is solved for a potential in two manners. That is, for an arbitrary given negative energy E, one is started at the small x_s taken to be $x_s = -\ln Z - 10$ using $Y(x_s) = e^{(l+1/2)x_s}$ and another is at the large x_L equal to $\ln r_L$, where $r_L = 25/(-E)^{1/2}$, using $Y(x_L) = \exp(x_L/2 - 25)$. When the logarithmic derivatives of these two solutions at a appropriate position x_0 connect continuously, the E is the energy eigenvalue for the potential. The x_0 is the larger one of two x, at which $\gamma(x)$ changes the sign. For $x < x_0$, the radial wave function $Y(x)$ oscillates because of presence of negative region of $\gamma(x)$, and for $x > x_0$ they show the exponential damping with a constant sign because of $\gamma(x) > 0$. The x_0 is the inflection point. For the continuous connection, it is convenient to use the logarithmic derivative since the normalizations of wave functions are not needed. For the numerical calculations of the derivative, the following formula is used.

$$\frac{dY}{dx} = \frac{1}{60h}\left[16\left(1-\frac{3}{4}h^2\gamma_1\right) Y_1 - 16\left(1-\frac{3}{4}h^2\gamma_{-1}\right) Y_{-1} + 7(Y_2 - Y_{-2})\right], \tag{26}$$

where h is the mesh interval and $h = 0.03$, $Y = Y(x)$, $Y_{\pm m} = Y(x \pm mh)$ and $\gamma_{\pm 1} = \gamma(x \pm h)$.

The acceptable energy eigenvalues and the wave functions are determined from the iteration in the self-consistent method. That is, if they are once obtained for the potential $V_i(r)$ in i-th iteration, the new potential $V_{i+1}(r)$ for the next step iteration is constructed from a mixing between the old potential $V_i(r)$ and the output potential $V_i^{(0)}(r)$ calculated using the wave functions obtained from $V_i(r)$. $V_{i+1}(r)$ is given by

$$V_{i+1}(r) = aV_i(r) + (1-a) V_i^{(0)}(r). \tag{27}$$

The mixing parameter is taken to be $a = 0.7$. The convergence of iteration is judged by the condition $|r[V_i(r) - V_i^{(0)}(r)]| < \varepsilon$ with $\varepsilon = 5\times 10^{-4}$. As the initial potential in iteration, the Hydrogen-like potential $-2Z/r$ is used. For these parameters, it takes about 34 iteration times for convergence.

4. Numerically calculated results and discussions

4.1 *Energy Eigenvalues*

The accuracies of the numerical calculations are first described. For this check, we used the results due to Moruzzi, Janak and Williams [8]. They calculated the total energy using the B-H exchange correlation energy, and, for example, for Fe atom, they obtained the lowest total energy $E_{total} = -2522.369$ Ryd for the configuration $3d_{\uparrow}{}^{5}3d_{\downarrow}{}^{1.4}4s_{\uparrow}{}^{1}4s_{\downarrow}{}^{0.6}$. We obtained $E_{total} = -2522.367$ Ryd for the same configuration. The agreement is very much excellent. For other atoms from Sc to Cu, we also did the check. The agreement were very much excellent for all atoms. Therefore, the accuracies of our calculations are very much good.

In Table I, the energy levels and the total energy are tabulated for the case of no inclusion of spin polarization, in which the electron numbers with the up and down spins are equal for each state. This case is referred to as the paramagnetic case below. The same configurations as those determined from the experiments are used in the calculations. Furthermore, the various exchange and the exchange-correlation effects are compared. We can immediately realize from Table I and Fig. 1 that the depth of each energy level depends on the exchange (-correlation) energies and is deepest for S exchange potential and most shallow for K-S one. The order of depth is arranged according to S, G-L, B-H and K-S. The results due to B-H and G-L are very close. For Cr and Cu, the energy levels of 3d and 4s states are very shallow compared to the neighboring atoms. This is due to the configuration. When the configurations $3d^4 4s^2$ for Cr and $3d^9 4s^2$ for Cu are used, these strange behaviors disappear. Furthermore, for atoms except for Sc, Ti and Cr, the energy levels for 3d state are deeper than 4s state. For Sc and

Table I The energy levels of 3d-transition atoms for the paramagnetic states are compared for various exchange (-correlation) potentials. S and K-S mean Slater and Kohn-Sham exchange potentials, and B-H and G-L, respectively, Barth-Hedin and Gunnarsson-Lundqvist exchange-correlation potentials.

		$-E_{1s}$	$-E_{2s}$	$-E_{2p}$	$-E_{3s}$	$-E_{3p}$	$-E_{3d}$	$-E_{4s}$	$-E_{total}$
Sc	K-S	320.20	34.292	28.356	3.8823	2.3736	0.17989	0.25127	1514.002
$3d^1 4s^2$	B-H	320.36	34.410	28.477	3.9804	2.4703	0.26747	0.31977	1517.310
21	G-L	320.40	34.437	28.505	3.9971	2.4863	0.27955	0.32430	1518.107
	S	326.24	35.914	30.071	4.3731	2.8261	0.47790	0.37416	1549.546
Ti	K-S	354.39	38.797	32.448	4.4214	2.7526	0.25487	0.27037	1690.997
$3d^2 4s^2$	B-H	354.54	38.914	32.568	4.5198	2.8500	0.34526	0.34113	1694.499
22	G-L	354.58	38.939	32.595	4.5363	2.8659	0.35813	0.34621	1695.349
	S	360.72	40.465	34.224	4.9239	3.2192	0.57455	0.39906	1729.379
V	K-S	390.28	43.512	36.749	4.9580	3.1263	0.32143	0.28620	1879.593
$3d^3 4s^2$	B-H	390.44	43.629	36.868	5.0577	3.2251	0.41440	0.35890	1883.294
23	G-L	390.48	43.654	36.894	5.0744	3.2414	0.42806	0.36450	1884.198
	S	396.90	45.233	38.591	5.4793	3.6132	0.66389	0.42099	1920.951
Cr	K-S	427.62	48.128	40.950	5.2171	3.2278	0.16081	0.24139	2080.064
$3d^5 4s^1$	B-H	427.75	48.227	41.051	5.3029	3.3134	0.24214	0.30798	2083.986
24	G-L	427.79	48.245	41.072	5.3149	3.3252	0.25186	0.31173	2084.954
	S	434.38	49.754	42.711	5.6437	3.6241	0.41480	0.33787	2124.727
Mn	K-S	467.23	53.615	46.011	6.0544	3.8848	0.44061	0.31342	2292.706
$3d^5 4s^2$	B-H	467.38	53.732	46.130	6.1570	3.9868	0.53795	0.38927	2296.816
25	G-L	467.42	53.757	46.157	6.1746	4.0041	0.55307	0.39579	2297.835
	S	474.42	55.448	47.990	6.6206	4.4182	0.82860	0.45978	2340.425
Fe	K-S	508.29	59.011	50.981	6.6208	4.2753	0.49559	0.32577	2517.774
$3d^6 4s^2$	B-H	508.44	59.129	51.102	6.7249	4.3789	0.59482	0.40296	2522.093
26	G-L	508.48	59.153	51.128	6.7430	4.3966	0.61060	0.40988	2523.171
	S	515.76	60.902	53.030	7.2108	4.8330	0.90600	0.47755	2568.881
Co	K-S	551.07	64.641	56.182	7.2016	4.6752	0.54834	0.33757	2755.547
$3d^7 4s^2$	B-H	551.22	64.758	56.302	7.3072	4.7803	0.64932	0.41599	2760.078
27	G-L	551.26	64.783	56.328	7.3257	4.7986	0.66572	0.42329	2761.217
	S	558.83	66.588	58.299	7.8159	5.2575	0.98090	0.49458	2810.182
Ni	K-S	595.58	70.505	61.613	7.7979	5.0854	0.59924	0.34896	3006.297
$3d^8 4s^2$	B-H	595.73	70.623	61.734	7.9049	5.1919	0.70184	0.42852	3011.044
28	G-L	595.77	70.648	61.760	7.9239	5.2107	0.71883	0.43618	3012.246
	S	603.62	72.510	63.798	8.4366	5.6924	1.05367	0.51101	3064.603
Cu	K-S	641.42	76.177	66.853	8.0215	5.1254	0.31548	0.27711	3270.454
$3d^{10} 4s^1$	B-H	641.57	76.283	66.962	8.1193	5.2230	0.40989	0.35125	3275.441
29	G-L	641.60	76.303	66.984	8.1349	5.2385	0.42379	0.35722	3276.714
	S	649.61	78.089	68.955	8.5668	5.6413	0.67746	0.40028	3332.849

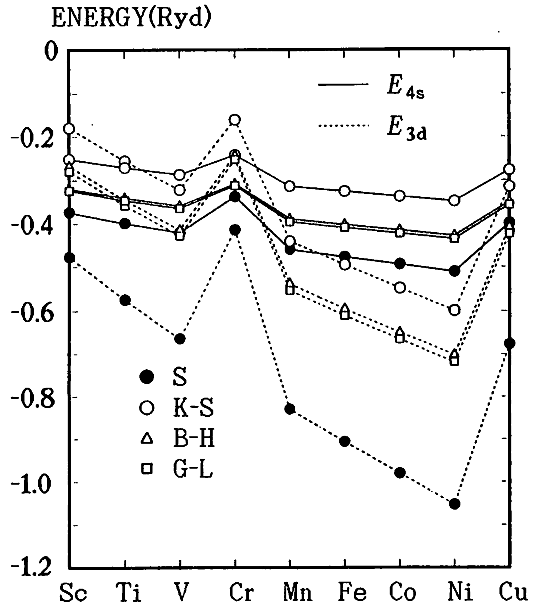

Fig. 1 The energy levels for the paramagnetic 3d and 4s states are plotted as a function of 3d-transition atom series, and compared for the various exchange (-correlation) potentials. Data in Table I are used.

Cr, the relation is reversed although it is different for S exchange potential. For Ti, both levels are almost same.

Next let us consider the energy levels and the total energy for the case including the spin polarization. Below, this case is referred to as the ferromagnetic case. These are shown in Table II and Fig. 2. There, the same atomic configurations as the paramagnetic case are used. However, the electron numbers in 3d and 4s states depend on the spin, although the equal numbers are assumed for the states from 1s to 3p. The numbers are distributed so as to have the maximum total spin for 3d and 4s states within the above given configuration, which is one of the Hund rule. For example, the configuration of Cr is $3d_{\uparrow}{}^{5}3d_{\downarrow}{}^{0}4s_{\uparrow}{}^{1}4s_{\downarrow}{}^{0}$. In Table II, the exchange (-correlation) potential effects are compared. In Fig. 2(a), the energy levels for 3d and 4s states are indicated only for the B-H exchange-correlation energy. It can be realized for all atoms by comparing Tables I and II that the total energies get lower by taking into account the spin polarization. This fact means that the 3d transition atoms will have a magnetic character, and support that these atoms have a strong magnetic properties by the crystallization. It follows from comparison between Fig. 1 and Fig. 2(a) that the splittings due to the spin occur for both 3d and 4s states, and, as naturally predicted, the spin up levels become deeper than the paramagnetic case and the spin down levels become more shallow. The magnitude of the splittings mainly depend on the difference between the electron numbers of the spin up and down in 3d states. Therefore, they are large for atoms near Cr. For this reason, for Cr, the spin down 3d state is pushed upward and this is no more a bound state. However, this is not contradict with the configuration of Cr because its state is empty. The energy levels shown in Fig. 2(a) are also consistent with the atomic configurations assumed for all atoms. That is, for atoms having the empty state, the states are most shallow.

Fig. 2(b) indicates the result obtained by adding the effect of Latter correction on Fig. 2(a). Its effect makes each level low. Other large effects are not observed.

Table II The energy levels of 3d-transition atoms with the spin polarizations are compared for various exchange (-correlation) potentials. The meanings of S, K-S, B-H and G-L are the same as in Table I.

			$-E_{1s}$	$-E_{2s}$	$-E_{2p}$	$-E_{3s}$	$-E_{3p}$	$-E_{3d}$	$-E_{4s}$	$-E_{total}$
	K-S	↑	320.20	34.295	28.357	3.9091	2.4009	0.20633	0.26579	1514.017
Sc		↓	320.20	34.276	28.342	3.8440	2.3351	0.14494	0.23424	1514.017
	B-H	↑	320.35	34.413	28.478	4.0033	2.4933	0.28862	0.33001	1517.323
$3d_{\uparrow}{}^{1}3d_{\downarrow}{}^{0}$		↓	320.35	34.396	28.464	3.9475	2.4376	0.23898	0.30727	1517.323
$4s_{\uparrow}{}^{1}4s_{\downarrow}{}^{1}$	G-L	↑	320.39	34.440	28.506	4.0199	2.5092	0.30051	0.33414	1518.120
		↓	320.39	34.423	28.492	3.9644	2.4539	0.25140	0.31225	1518.120
21	S	↑	326.24	35.926	30.079	4.4260	2.8789	0.52745	0.39367	1549.573
		↓	326.24	35.889	30.050	4.3083	2.7617	0.41865	0.35279	1549.573
	K-S	↑	354.37	38.801	32.447	4.4761	2.8076	0.30692	0.29462	1691.062
Ti		↓	354.37	38.753	32.410	4.3313	2.6632	0.17614	0.24067	1691.062
	B-H	↑	354.52	38.917	32.566	4.5657	2.8957	0.38698	0.35829	1694.553
$3d_{\uparrow}{}^{2}3d_{\downarrow}{}^{0}$		↓	354.52	38.873	32.532	4.4415	2.7730	0.27930	0.31827	1694.553
$4s_{\uparrow}{}^{1}4s_{\downarrow}{}^{1}$	G-L	↑	354.57	38.943	32.594	4.5819	2.9113	0.39942	0.36281	1695.402
		↓	354.57	38.899	32.559	4.4587	2.7897	0.29289	0.32395	1695.402
22	S	↑	360.69	40.485	34.234	5.0268	3.3213	0.66986	0.43260	1729.491
		↓	360.69	40.395	34.165	4.7780	3.0754	0.44474	0.36041	1729.491
	K-S	↑	390.25	43.517	36.743	5.0397	3.2079	0.39816	0.31830	1879.747
V		↓	390.25	43.431	36.678	4.8078	2.9783	0.19266	0.24609	1879.747
	B-H	↑	390.40	43.631	36.861	5.1258	3.2926	0.47621	0.38171	1883.423
$3d_{\uparrow}{}^{3}3d_{\downarrow}{}^{0}$		↓	390.40	43.552	36.801	4.9259	3.0962	0.30441	0.32698	1883.423
$4s_{\uparrow}{}^{1}4s_{\downarrow}{}^{1}$	G-L	↑	390.44	43.657	36.888	5.1420	3.3083	0.48921	0.38663	1884.326
		↓	390.44	43.578	36.828	4.9439	3.1138	0.31920	0.33321	1884.326
23	S	↑	396.85	45.259	38.598	5.6289	3.7611	0.80230	0.46596	1921.211
		↓	396.86	45.105	38.482	5.2408	3.3791	0.45458	0.36746	1921.211
	K-S	↑	427.51	48.094	40.900	5.2940	3.3052	0.24003	0.30215	2080.547
Cr		↓	427.51	47.954	40.793	4.9360	2.9476		0.02000	2080.547
	B-H	↑	427.66	48.195	41.005	5.3689	3.3792	0.30709	0.35213	2084.385
$3d_{\uparrow}{}^{5}3d_{\downarrow}{}^{0}$		↓	427.66	48.065	40.906	5.0557	3.0688		0.13393	2084.385
$4s_{\uparrow}{}^{1}4s_{\downarrow}{}^{0}$	G-L	↑	427.70	48.214	41.026	5.3803	3.3904	0.31596	0.35418	2085.347
		↓	427.69	48.084	40.926	5.0694	3.0825		0.14725	2085.347
24	S	↑	434.24	49.734	42.661	5.8057	3.7853	0.57351	0.44083	2125.524
		↓	434.24	49.486	42.474	5.2039	3.1876		0.01842	2125.524
	K-S	↑	467.15	53.617	45.992	6.1859	4.0155	0.56385	0.35856	2293.166
Mn		↓	467.15	53.435	45.854	5.7662	3.6024	0.19677	0.25603	2293.166
	B-H	↑	467.31	53.729	46.109	6.2668	4.0953	0.63850	0.42164	2297.210
$3d_{\uparrow}{}^{5}3d_{\downarrow}{}^{0}$		↓	467.30	53.561	45.981	5.9006	3.7367	0.32425	0.34152	2297.210
$4s_{\uparrow}{}^{1}4s_{\downarrow}{}^{1}$	G-L	↑	467.35	53.754	46.135	6.2834	4.1115	0.65250	0.42729	2298.225
		↓	467.35	53.587	46.008	5.9206	3.7563	0.34130	0.34859	2298.225
25	S	↑	474.31	55.480	47.986	6.8549	4.6496	1.04715	0.52372	2341.188
		↓	474.31	55.167	47.750	6.1721	3.9792	0.43902	0.38070	2341.188
	K-S	↑	508.24	59.042	50.994	6.7510	4.4037	0.61383	0.35947	2518.078
Fe		↓	508.24	58.879	50.870	6.4030	4.0621	0.30998	0.28759	2518.078
	B-H	↑	508.40	59.154	51.110	6.8357	4.4877	0.69387	0.42848	2522.356
$3d_{\uparrow}{}^{5}3d_{\downarrow}{}^{1}$		↓	508.39	59.003	50.995	6.5311	4.1898	0.43151	0.37080	2522.356
$4s_{\uparrow}{}^{1}4s_{\downarrow}{}^{1}$	G-L	↑	508.44	59.178	51.136	6.8526	4.5043	0.70850	0.43488	2523.431
		↓	508.44	59.029	51.022	6.5509	4.2094	0.44872	0.37799	2523.431
26	S	↑	515.70	60.968	53.063	7.4298	5.0484	1.10706	0.52459	2569.381
		↓	515.70	60.690	52.854	6.8689	4.4985	0.60718	0.42441	2569.381
	K-S	↑	551.05	64.682	56.207	7.3132	4.7850	0.64839	0.36119	2755.722
Co		↓	551.04	64.548	56.105	7.0455	4.5225	0.41398	0.31239	2755.722
	B-H	↑	551.20	64.795	56.324	7.4037	4.8749	0.73485	0.43461	2760.231
$3d_{\uparrow}{}^{5}3d_{\downarrow}{}^{2}$		↓	551.20	64.671	56.230	7.1683	4.6447	0.53085	0.39469	2760.231
$4s_{\uparrow}{}^{1}4s_{\downarrow}{}^{1}$	G-L	↑	551.24	64.819	56.350	7.4212	4.8921	0.75030	0.44163	2761.369
		↓	551.24	64.696	56.256	7.1882	4.6643	0.54829	0.40213	2761.369
27	S	↑	558.80	66.664	58.347	7.9988	5.4371	1.14775	0.52737	2810.470
		↓	558.80	66.438	58.177	7.5699	5.0168	0.76390	0.45953	2810.470
	K-S	↑	595.57	70.542	61.639	7.8799	5.1659	0.67229	0.36376	3006.377
Ni		↓	595.57	70.446	61.566	7.6979	4.9874	0.51214	0.33372	3006.377
	B-H	↑	595.72	70.657	61.758	7.9767	5.2622	0.76524	0.44055	3011.114
$3d_{\uparrow}{}^{5}3d_{\downarrow}{}^{3}$		↓	595.72	70.568	61.690	7.8158	5.1049	0.62489	0.41560	3011.114
$4s_{\uparrow}{}^{1}4s_{\downarrow}{}^{1}$	G-L	↑	595.76	70.682	61.784	7.9950	5.2803	0.78157	0.44807	3012.315
		↓	595.76	70.593	61.716	7.8357	5.1245	0.64257	0.42333	3012.315
28	S	↑	603.61	72.575	63.844	8.5689	5.8222	1.17401	0.53149	3064.733
		↓	603.61	72.413	63.722	8.2785	5.5375	0.91275	0.48986	3064.733
	K-S	↑	641.42	76.166	66.843	8.0107	5.1155	0.31493	0.31767	3270.479
Cu		↓	641.41	76.172	66.847	8.0187	5.1218	0.30238	0.21052	3270.479
	B-H	↑	641.56	76.276	66.955	8.1125	5.2168	0.41030	0.38062	3275.459
$3d_{\uparrow}{}^{5}3d_{\downarrow}{}^{5}$		↓	641.56	76.279	66.957	8.1158	5.2189	0.39914	0.30398	3275.459
$4s_{\uparrow}{}^{1}4s_{\downarrow}{}^{0}$	G-L	↑	641.60	76.296	66.977	8.1284	5.2326	0.42425	0.38534	3276.732
		↓	641.60	76.299	66.979	8.1311	5.2341	0.41307	0.31254	3276.732
29	S	↑	649.60	78.072	68.940	8.5506	5.6267	0.67614	0.47326	3332.894
		↓	649.60	78.084	68.949	8.5644	5.6375	0.65990	0.27511	3332.894

4.2 *Potentials*

Here we describe the potential given by (7), which is the sum of the nucleus, the electronic Coulomb (Hartree) and the exchange (-correlation) potentials. This is obtained finally by the convergence of iteration in the self-consistent calculation. The potentials are shown

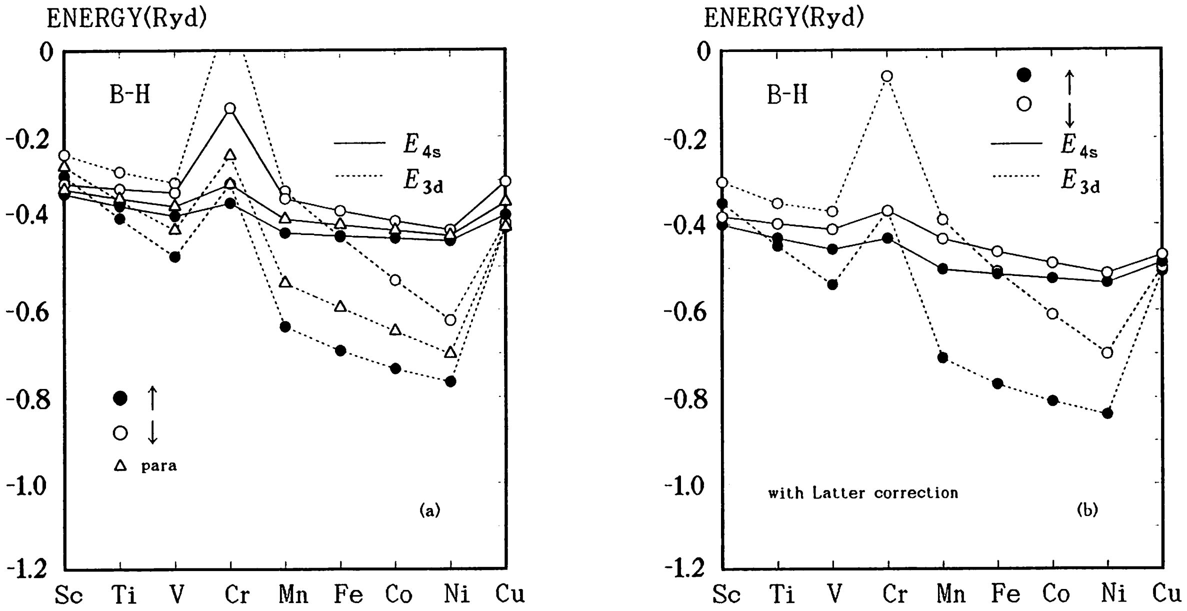

Fig. 2 The energy levels for the ferromagnetic 3d and 4s states are shown as a function of the 3d-transition atom series, and compared to the paramagnetic case. The energy level data for the B-H exchange-correlation potential in Table I and Table II are used. (a) without Latter correction, (b) with Latter correction.

in Fig. 3 for Sc, Cr, Fe and Cu. In Fig. 3, the potentials for the paramagnetic case and for the spin up and down in the ferromagnetic case are compared. They are very different from the initial potential $-2Z/r$ in the iteration. Fig. 3 tells us that the deviations of the potentials for the ferromagnetic case from those for the paramagnetic case are not so large compared to our prediction. But as mentioned above, this not so large change of the potential makes the large change on the energy levels. Therefore, the energy levels are very much sensitive to the potential. Particularly, the difference between the potentials for the paramagnetic and the ferromagnetic cases is very small for Fe. On the other hand, except for Sc, the differences in the region of small r between both cases almost do not exist, and their differences occur in the region $r > 1.5$ a.u. For Sc, the potential for the paramagnetic case is deepest in the three kinds of potentials for $r > 1$ a.u. However, for $r < 1$ a.u., the potential is most shallow. The deepest character for $r > 1$ a.u. is compensated by this most shallow potential for $r < 1$ a.u. This behavior is not observed for other atoms.

4.3 Surface charge density

The spin dependent surface charge density is given by

$$\sigma(r) = 4\pi r^2 \rho_\sigma(r) = \sum_{nl} n_{nl\sigma} r^2 R_{nl\sigma}{}^2(r) \qquad (28)$$

where $R_{nl\sigma}(r)$ is a solution of eq. (10) and $n_{nl\sigma}$ is the occupation electron numbers. The computed density $\sigma(r)$ is shown in Fig. 4 as a function of r for Sc, Cr, Fe and Cu. Sum with respect to spin followed by integration with respect to r of $\sigma(r)$ gives the total electron numbers Z. The total density $\sigma(r)$ is decomposed into two parts $\sigma_{1s-3p}(r)$ and $\sigma_{3d-4s}(r)$, in which $\sigma(r) = \sigma_{1s-3p}(r) + \sigma_{3d-4s}(r)$. $\sigma_{1s-3p}(r)$ is the density due to the electrons occupying the states from 1s to 3p, and $\sigma_{3d-4s}(r)$ is from 3d to 4s. These quantities depend on the spin. In Fig. 4, these three kinds of densities are indicated, and the corresponding densities for the paramagnetic case per spin are also shown for comparison. All densities are calculated using the B-H exchange-correlation potential.

At first, we must note that $\sigma_{1s-3p}(r)$ almost does not depend on the spin and damps rapidly. Their values are zero for $r > 2.7$ a.u. even for Sc showing the most slowly damping. When these atoms make the crystal, the muffin-tin radius r_{MT}

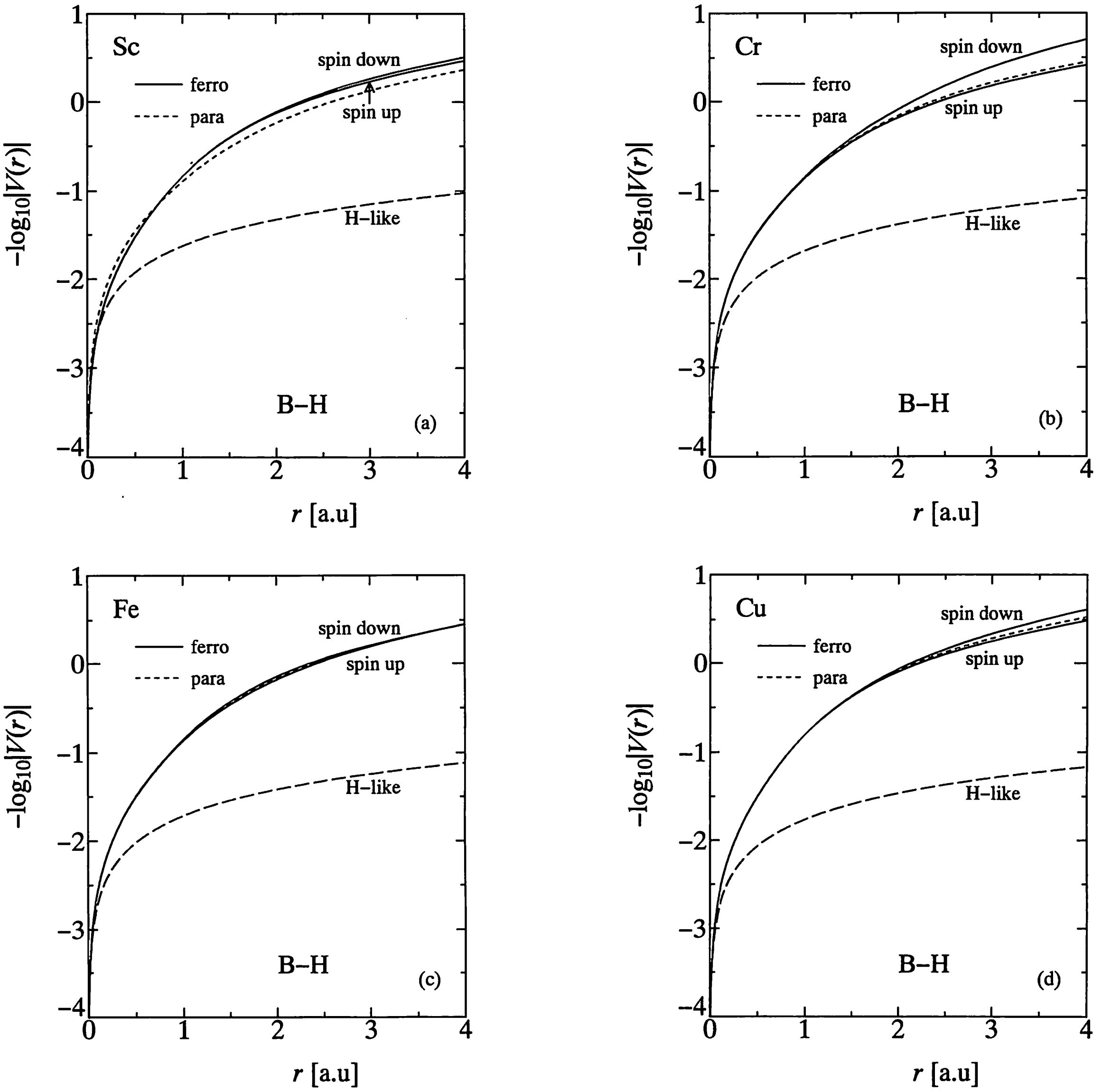

Fig. 3 The potentials obtained from the self-consistent calculations, in which the B-H potential is used for the exchange-correlation potential, are shown as a function of r. "ferro" and "para" mean the ferromagnetic and the paramagnetic cases, respectively. "H-like" is the Hydrogen-like potential -2Z/r. (a) Sc, (b) Cr, (c) Fe and (d) Cu.

in the APW theory, equal to half of the nearest neighbor distance, is 3 a.u for Sc, 2.3 a.u for Cr, 2.23 for Fe and 2.39 for Cu. For these four atoms, $\sigma_{1s-3p}(r)$ are almost zero for $r > r_{MT}$. Therefore, when they make the solid, the electrons from 1s to 3p stay inside of the muffin-tin sphere.

Next let us consider $\sigma_{3d-4s}(r)$. For Cu, since the electron numbers in 3d states are five for both up and down spins, its spin dependence is very weak particularly for small r. However, for $r >$ 2 a.u, its dependence appears clearly. For other atoms, the spin dependences are almost determined by the difference between the electron numbers with the spin up and down for the given atomic configuration. Note that there are no electrons with the spin down for Cr. It is important to note that the 3d and 4s electrons with the spin polarization exist beyond the muffin-tin radius. This leads that these electrons form the conduction bands by the crystallization and their spin polarizations give an origin of the strong magnetism observed in the experiments.

Since the total surface densities are the sum of $\sigma_{1s-3p}(r)$ and $\sigma_{3d-4s}(r)$, their behaviors are easily understood from Fig. 4.

Last, we give a comment. It is that the

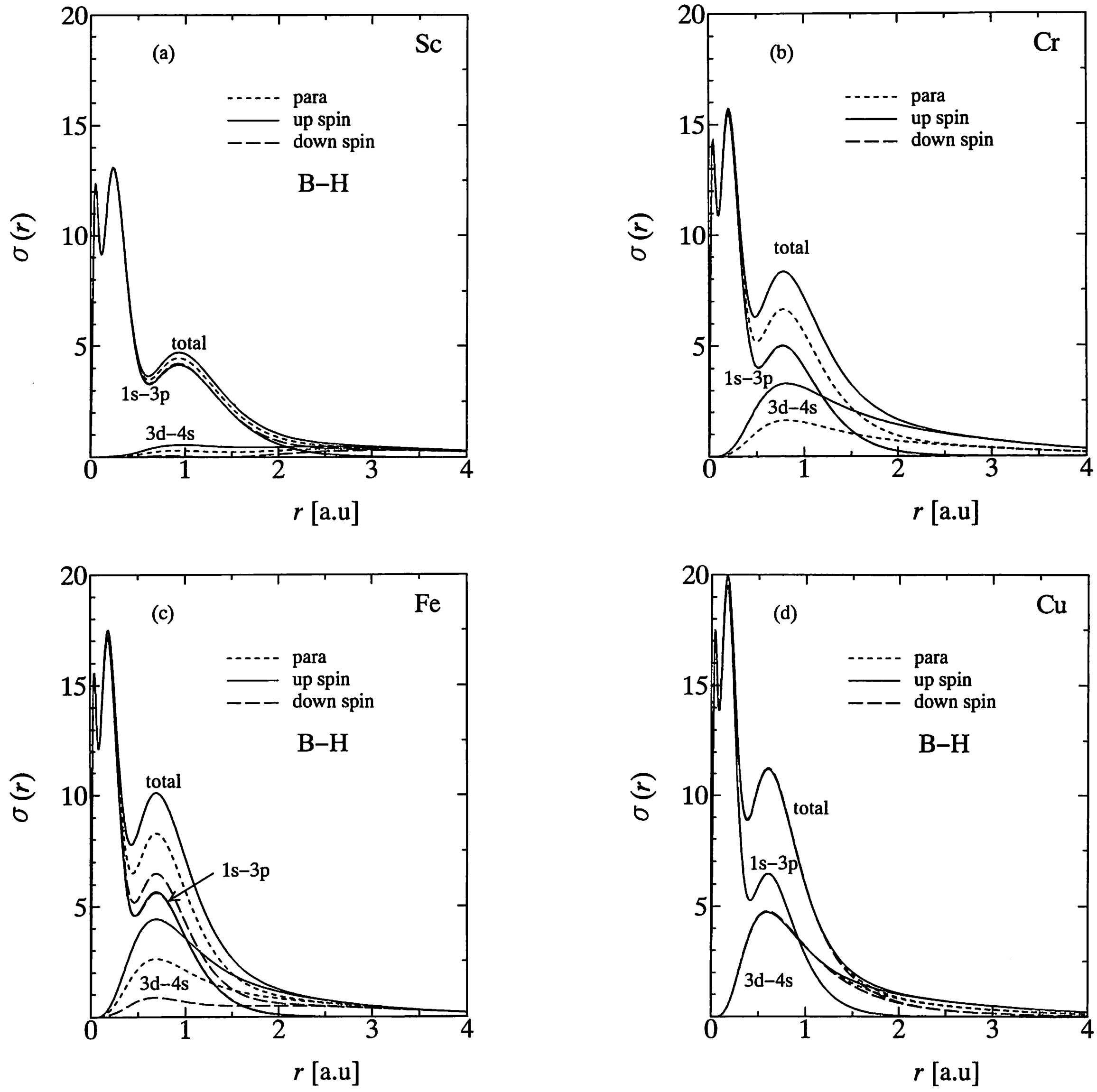

Fig. 4 The three kinds of the surface charge densities $\sigma_{1s-3p}(r)$, $\sigma_{3d-4s}(r)$ and $\sigma_{total}(r)$ are shown as functions of r for the ferromagnetic and the paramagnetic cases. Note that those per spin are indicated for the paramagnetic case. The B-H exchange-correlation is used for these calculations. (a) Sc, (b) Cr, (c) Fe and (d) Cu.

surface charge densities are not so sensitive to the potential compared to the energy eigenvalues mentioned above. This can be roughly seen from the comparison between Fig. 3 and Fig. 4.

5. Conclusion

We found that the energy levels and potentials are sensitive to both the exchange-correlation energies and the spin polarized configuration. The total energies become lower by taking into account the spin polarizations. This support that the 3d-transition atoms show the strong magnetic properties by the crystallizations. The assumptions that the 1s to 3p electrons can be treated as the frozen core state and the 3d to 4s electrons become the band electrons are justified. Accordingly, these 3d and 4s electrons can make the spin polarized energy band structure by the crystallizations.

Appendix : Electronic Coulomb Potential in APW theory

One of authors wrote the wrong expressions in ref. [3]. They are eqs.(43) and (44). The eq.

(44) must be corrected as follows,

$$V_0 = \frac{1}{\Omega - \sum_s \Omega_s} \sum_s \Omega_s \left(\frac{3Q_s}{a_s} + \frac{4\pi\bar{\rho}}{5} a_s^2 - V_{Ms}(0) \right) \tag{A1}$$

This expression can be derived in the following way. The average potential V_0 outside the muffin-tin spheres can be calculated by

$$V_0 = \frac{1}{\Omega - \sum_s \Omega_s} \int_{\Omega_{out}} V(\boldsymbol{r})\, d\boldsymbol{r}, \tag{A2}$$

where $V(\boldsymbol{r})$ is the potential outside the spheres. Because $V(\boldsymbol{r})$ is the same for both A-charge and fictious charge models, it is easy to use $V(\boldsymbol{r})$ due to the fictious model. The following calculations are straightforward although long.

References

[1] A. Hasegawa, Japanese Journal of Applied Physics, 8 (1993) 162.

[2] J.C. Slater, Phys. Rev. **51** (1937) 846.

[3] A. Narita and K. Sato, Research Reports of Akita National College of Technology, **30** (1994) 187.

[4] F. Herman and S. Skillman, "Atomic Structure Calculations", Printice-Hall (1963).

[5] J.C. Slater, "The Calculation of Molecular Orbitals", John Wiley & Sons, Inc. (1979).

[6] W. Kohn and L.J. Sham, Phys. Rev. **140** (1965) A1133.

[7] P. Hohenberg and W. Kohn, Phys. Rev. **136** (1964) B864.

[8] V.L. Moruzzi, F.F. Janak and A.R. Williams, "Calculated Electronic Properties of Metals", Pergamon Press Inc. (1978).

[9] O. Gunnarsson and B.I. Lundqvist, Phys. Rev. **B13** (1976) 4274.

[10] O.v. Barth and L. Hedin, J. Phys. **C5** (1972) 1629.

[11] L. Hedin and B.I. Lundqvist, J. Phys. **C4** (1971) 2064.

[12] K.S. Singwi and A. Sjolander, M.P. Tosi, R.H. Land, Phys. Rev. **B1** (1970) 1044.

[13] J.B. Mann, Los Alamos Scientific Laboratory Report, LA-3690 (1967).

[14] V. Kumar, O.K. Anderson, A. Mookerjee, "Lectures on Methods of Electric Structure Calculations", ICTP (1992).

[15] T.L. Loucks, "Augmented Plane Wave Method", Benjamin (1967).